

# UV and Sunlight Driven Photoligation of Quantum Dots: Understanding the Photochemical Transformation of the Ligands

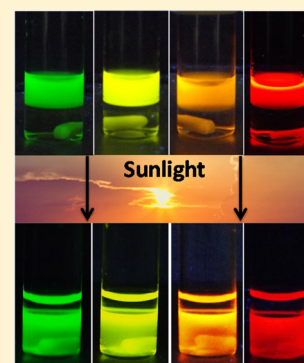
Fadi Aldeek,<sup>†</sup> Dana Hawkins,<sup>†</sup> Valle Palomo,<sup>‡</sup> Malak Safi,<sup>†</sup> Goutam Palui,<sup>†</sup> Philip E. Dawson,<sup>‡</sup> Igor Alabugin,<sup>†</sup> and Hedi Mattoussi<sup>\*†</sup>

<sup>†</sup>Department of Chemistry and Biochemistry, Florida State University, 95 Chieftan Way, Tallahassee, Florida 32306, United States

<sup>‡</sup>Department of Chemistry and Department of Cell Biology, The Scripps Research Institute, 10550 N. Torrey Pines Road, La Jolla, California 92037, United States

**S** Supporting Information

**ABSTRACT:** We have recently reported that photoinduced ligation of ZnS-overcoated quantum dots (QDs) offers a promising strategy to promote the phase transfer of these materials to polar and aqueous media using multidentate lipoic acid (LA)-modified ligands. In this study we investigate the importance of the underlying parameters that control this process, in particular, whether or not photoexcited QDs play a direct role in the photoinduced ligation. We find that irradiation of the ligand alone prior to mixing with hydrophobic QDs is sufficient to promote ligand exchange. Furthermore, photoligation onto QDs can also be carried out simply by using sunlight. Combining the use of Ellman's test with matrix-assisted laser desorption/ionization and electrospray ionization mass spectrometry, we probe the nature of the photochemical transformation of the ligands. We find that irradiation (using either a UV photoreactor or sunlight) alters the nature of the disulfide groups in the lipoic acid, yielding a different product mixture than what is observed for chemically reduced ligands. Irradiation of the ligand in solution generates a mixture of monomeric and oligomeric compounds. Ligation onto the QDs selectively favors oligomers, presumably due to their higher coordination onto the metal-rich QD surfaces. We also show that photoligation using mixed ligands allows the preparation of reactive nanocrystals. The resulting QDs are coupled to proteins and peptides and tested for cellular staining. This optically controlled ligation of QDs combined with the availability of a variety of multidentate and multifunctional LA-modified ligands open new opportunities for developing fluorescent platforms with great promises for use in imaging and sensor design.



## INTRODUCTION

The unique and controllable photophysical properties of semiconductor nanocrystals (quantum dots, QDs) have generated great interest among physicists, chemists, engineers, and biologists alike, because they offer a set of interesting fundamental concepts to understand along with a great potential for applications in electronic devices, biological imaging, sensing, and clinical diagnostics.<sup>1–5</sup> These properties include tunable and narrow fluorescence emission, broad absorption profiles, high brightness and superior photo- and chemical stability.<sup>6–12</sup>

High-quality QDs with crystalline cores, low size dispersity, and high fluorescence quantum yield are routinely prepared using high-temperature reduction of organometallic precursors in a mixture of coordinating solvents such as tri-*n*-octylphosphine/tri-*n*-octylphosphine oxide (TOP/TOPO), alkylamine, and alkylphosphonic acids.<sup>13–18</sup> The resulting materials are capped with hydrophobic ligands and are thus dispersible only in organic solvents. An effective phase-transfer strategy is therefore required to facilitate their integration with biological systems. One of the commonly explored strategies to achieve this goal relies on replacing the native cap with hydrophilic bifunctional ligands (cap/ligand exchange). To be effective, this approach requires the use of hydrophilic ligands

with strong coordination onto the metal surface of the nanocrystals in order to achieve complete removal of the hydrophobic cap and produce stable nanocrystals in biological media.<sup>3,19–21</sup>

Multidentate thiolated ligands provide enhanced stability to QDs in aqueous media, due to the higher ligand-to-nanocrystal affinity afforded by the simultaneous coordination of multiple thiols onto the same QD surface. In particular, dihydrothiolated lipoic acid (DHHLA)-based ligands were shown to impart better colloidal stability to the QDs over a wide range of biological conditions than their monothiol-appended counterparts.<sup>22,23</sup> The biocompatibility and functionality of QDs stabilized with DHHLA-based ligands have been enhanced through insertion of polyethylene glycol or/and zwitterionic moieties into the ligand structure. Further modification of the lipoic acid (LA) ligand has also allowed the controllable introduction of inert (OCH<sub>3</sub>) and reactive functional groups (e.g., carboxyl, amine, azide) into the organic surface coating of the nanocrystal.<sup>20,24–27</sup>

Cap exchange of hydrophobic QDs with LA-modified ligands has thus far required the use of the reduced form of the ligands, i.e., DHHLA-based compounds. Reduction of the disulfide to

Received: December 16, 2014

Published: January 22, 2015

dithiol has been carried out chemically, using  $\text{NaBH}_4$  as a reducing agent.<sup>24</sup> Though effective, this route requires multiple steps and careful storage of the DHLA-based ligands. DHLA-modified compounds are not shelf stable and must be generated through reduction of the 1,2-dithiolane moiety of the LA precursors. Furthermore, borohydride reduction alters the integrity of certain sensitive but highly desirable functional groups for bioconjugation, such as azides and aldehydes.<sup>23,28,29</sup>

In order to address these problems, our group has taken into consideration the photosensitive nature of the cyclic disulfide in the ligands. It has been shown that UV irradiation of LA can produce a heterogeneous mixture of monomeric and polymeric complexes.<sup>30,31</sup> We have recently built on those findings and showed that ligand exchange on QDs can be promoted photochemically, starting from the oxidized form of the ligand. In particular, we have found that irradiation of the native TOP/TOPO-capped QDs in the presence of LA-PEG using a UV photoreactor can readily transfer the nanocrystals to polar solvents and, most importantly, to water.<sup>32</sup> Nonetheless, several questions are still left unanswered, including whether or not the photoexcited QDs play a role in the transformation of the LA groups, what is the nature of the photochemical transformation of the ligands, and whether or not the LA derivatives are reduced. In addition, we hoped to evaluate whether the strategy could be applied using simple sunlight instead of a laboratory UV photoreactor.

In the present work, we expand on the earlier findings by focusing on the role that the QDs may or may not play and seek a better understanding of the nature of the photochemical transformation of the ligands when irradiated in the absence of the QDs. We use a combination of UV-vis absorption spectroscopy, Ellman's assay/test along with matrix-assisted laser desorption/ionization (MALDI) and electrospray ionization (ESI) mass spectrometry measurements to identify the nature of the photochemical transformation with the lipoic acid. We then propose a rationale for why this strategy is highly effective for the transfer of QDs to polar solvents and buffer media.

## RESULTS AND DISCUSSION

In a previous report, we showed that cap exchange of LA-based ligands onto luminescent QDs can be induced photochemically using *in situ* irradiation of the oxidized form of the ligand in the presence of hydrophobic nanocrystals.<sup>32</sup> Here, activation of the disulfide, ligand exchange, and phase transfer of the nanocrystals were all combined in the same step. The photoinduced phase transfer was implemented using either a single phase (e.g., polar methanol) or a two-phase (polar methanol and hexane) reaction, starting with the hydrophobic QDs. This procedure has obviated the need for chemical reduction of the LA under harsh conditions using sodium borohydride prior to performing the ligand exchange, along with the requirements for storage of the reduced ligand under inert atmosphere.<sup>23</sup> This route has also been applied to various PEG- and zwitterion-modified mono- and bis(LA) ligands, producing dispersions of QDs with great colloidal stability and easy to integrate with biology.<sup>32–34</sup>

We attributed the success of this strategy to the sensitivity of the LA to UV-excitation (at 320–350 nm) with potential contribution from electron transfer to LA (from photoexcited QDs), facilitating the reduction of the disulfide and coupling onto the ZnS-overcoated QDs. Indeed, the cyclic disulfide of LA exhibits a well-defined broad absorption band centered at

~330 nm, which undergoes a progressive decrease to near zero after ~30–40 min irradiation using a UV signal at 350 nm. We suggested that a homolytic “cleavage” of the S–S bond in the LA occurs under UV excitation, which promotes ligand coordination onto the Zn-rich surface of the QDs. A side-by-side comparison of the  $^1\text{H}$  NMR spectra collected from photoirradiated and chemically reduced ligands indicated that the photochemical reaction results in a mixture of products with chemical shifts similar to both the oxidized LA (the starting material) and to the reduced DHLA. However, the signatures of some of the protons close to the dithiolane ring observed for the UV-irradiated ligands were different from those recorded for the borohydride-reduced compounds.<sup>32</sup>

In this study we wanted to develop an understanding of the photochemical transformation by addressing the following questions. (1) Do the QDs play an active role in the photochemical transformation of the LA groups and the ensuing cap exchange? (2) Can the phase transfer be implemented using TOP/TOPO-QDs mixed with ligands irradiated in the absence of QDs? (3) Can the phase transfer be implemented simply using sunlight exposure? (4) What is the chemical composition of the irradiated ligands and why is this route more effective than cap exchange using borohydride-reduced ligands?

**Irradiation of the Isolated Ligands Followed by QD Phase Transfer.** In this route, the LA-based ligands were first dissolved in methanol, irradiated for 30 min in a UV reactor (see Experimental Section), and then mixed with a hexane solution containing TOP/TOPO-QDs (i.e., two-phase configuration). After stirring the mixture at room temperature for 15 min, the QDs were fully transferred from hexane to methanol (Figure 1). Following evaporation of the solvent(s), the nanocrystals were dispersed in ethanol and then precipitated with hexane to remove excess/free ligands. The resulting QD pellet fully dispersed in water. Applying 2–3 rounds of purification, using a centrifugal filtration device to remove the remaining soluble ligands, provided homogeneous dispersions of QDs which could be stored for further use.

Alternatively, the preirradiated solution of ligands in methanol could be mixed with a solid precipitate of the hydrophobic QDs (i.e., one phase configuration). Stirring the mixture also promoted cap exchange and dispersion of the nanocrystals in methanol. The solution was processed as above, producing a homogeneous QD dispersion in water. The phase transfer using irradiated ligands was rapid, needing only ~15 min of mixing at room temperature. Importantly, this process required only about one-fifth of the excess ligand typically used for phase transfer with borohydride-reduced ligands. In addition, there was no need to heat the solutions in either one- or two-phase protocol, which contrasts with the need to heat the reaction mixture at 60 °C for several hours (6–12 h), when DHLA-PEG derivatives were used.<sup>23</sup>

We have applied this method to transfer four different sets of QDs emitting at 540 nm (green), 570 nm (yellow), 590 nm (orange), and 630 nm (red) (Figure 1). Figure 2A,B shows the absorption and emission spectra collected from these QDs before and after phase transfer. The hydrophilic QDs retained the photophysical properties of the starting nanocrystals, with a minimal spectroscopic shift in both absorption and photoluminescence; ~2–4 nm red shift was measured in some cases for dispersions in buffer media. Such a small shift has been occasionally measured for QDs following transfer to water media.<sup>24</sup> The photoluminescence (PL) quantum yields (QYs)

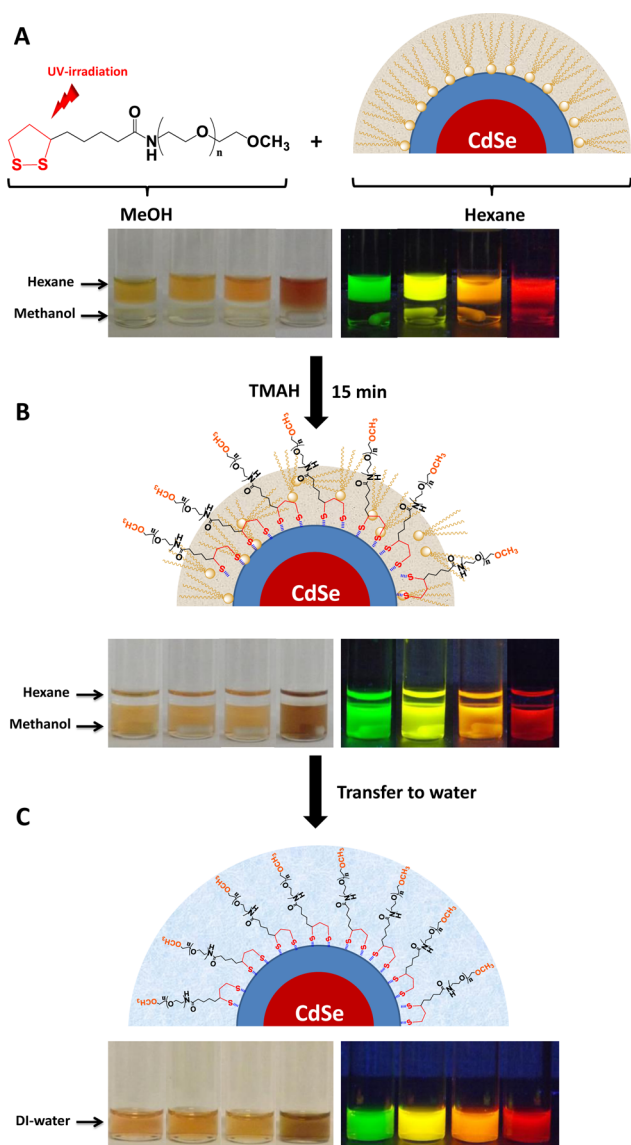


**Figure 1.** Schematic representation showing the cap exchange using preirradiated ligands. (A) Representation of the starting QDs and ligands along with white light and fluorescence images of a two-phase mixture of TOP/TOPO-QDs in hexane and preirradiated LA-PEG<sub>750</sub>-OCH<sub>3</sub> in methanol, immediately following mixing; four samples of distinct color QDs are shown. (B) Schematic representation of the QD ligation combined with white light and fluorescence images of the above two-phase solutions following phase transfer. (C) Schematics of the final hydrophilic PEG-capped QDs together with fluorescent images of these QDs in water. The dispersions were excited using hand-held UV lamp, with  $\lambda_{\text{exc}} = 365$  nm. The QD samples shown emit at 540 nm (green), 570 nm (yellow), 590 nm (orange), and 630 nm (red).

of LA-PEG<sub>750</sub>-OCH<sub>3</sub>-capped QDs in water were overall smaller than the native TOP/TOPO-capped nanocrystals dispersed in hexane (see Figure 2). For instance, starting with a QD sample having a QY of 40% in hexane produced water dispersion with QY of 20–30%. Such reduction in the PL emission is commonly observed following phase transfer to water, though decrease in the measured QYs for thiol-modified ligands is often slightly larger.<sup>35</sup> Importantly, the photophysical properties of QDs generated with irradiated ligands are nearly

identical to those exhibited by QDs previously prepared using chemically reduced DHLA.

Taken together, these findings prove that the QDs do not play a direct role in the photochemical transformation of the LA groups. They indicate that potential charge-transfer interactions from photoexcited QDs play no role in the phase-transfer process. As such, decreasing the QD size (i.e., shifting the emission location farther to the blue), which widens the band gap and shifts the exact location of the conduction and valence band energies, does not affect the ligation strategy. They also indicate that irradiating the ligand separately, then proceeding with the phase-transfer step(s) may be more beneficial, as this route consumes less ligands, does not even require mild sample heating, and avoids extended exposure of the QDs to UV irradiation.

**Sunlight-Mediated Ligation of the QDs.** We also carried out the phase transfer relying on the photochemical transformation of the ligand using sunlight exposure, instead of a laboratory UV reactor. Here, we tested the viability of this route using all three configurations: (1) sunlight irradiation of precipitated TOP/TOPO-QDs mixed with LA-PEG in methanol (one phase); (2) sunlight irradiation of a two-phase mixture using ligands in methanol and QDs in hexane; and (3) sunlight irradiation of the ligand in methanol followed by two-phase transfer. The main question we wanted to address is whether or not photoligation of QDs with LA-based ligands requires a laboratory UV reactor.

We found that the photochemical transformation of the ligands does not require a laboratory UV reactor and successful cap exchange of the QDs could be achieved in all three configurations mentioned above. Furthermore, the absorption and PL emission properties of the final QDs dispersed in buffer media using sunlight irradiation were very similar to those prepared using a UV reactor (see Supporting Information, Figure S1). Slight differences were observed, and in certain instances, the final quantum yield of QDs photoligated under sunlight irradiation was slightly higher than those prepared using a laboratory UV reactor (see Supporting Information, Figure S2). This enhanced QY may be attributed to the milder conditions of the photochemical transformation of the ligands using irradiation provided by simple sunlight exposure. We should also note that the observed decrease in the QY of the QDs following phase transfer with the ligands (compared to their hydrophobic counterparts) is attributed to the nature of the thiol coordination onto the metal surface of the nanocrystals, not to a partial (or inefficient) ligand exchange with the present strategy. In fact, independent preliminary estimates indicate that the ligand density measured for QDs capped with the chemically reduced DHLA-PEG is comparable to that measured for QDs photoligated with LA-PEG ligands (data not shown).

We expanded the use of the sunlight-mediated photoligation and phase transfer using zwitterion-modified LA (LA-ZW) ligands. We carried out phase transfer with LA-ZW using the configurations introduced above; we tested this route using two different sets of QDs (orange- and green-emitting) and applying 30 min irradiation periods for all samples. Here too, sunlight irradiation produced homogeneous QD dispersions with absorption and PL emission spectra that are similar to those of the TOPO/TOP-capped QDs (see Supporting Information, Figure S3). Phase transfer under sunlight exposure was also carried out using commercially available LA, yielding



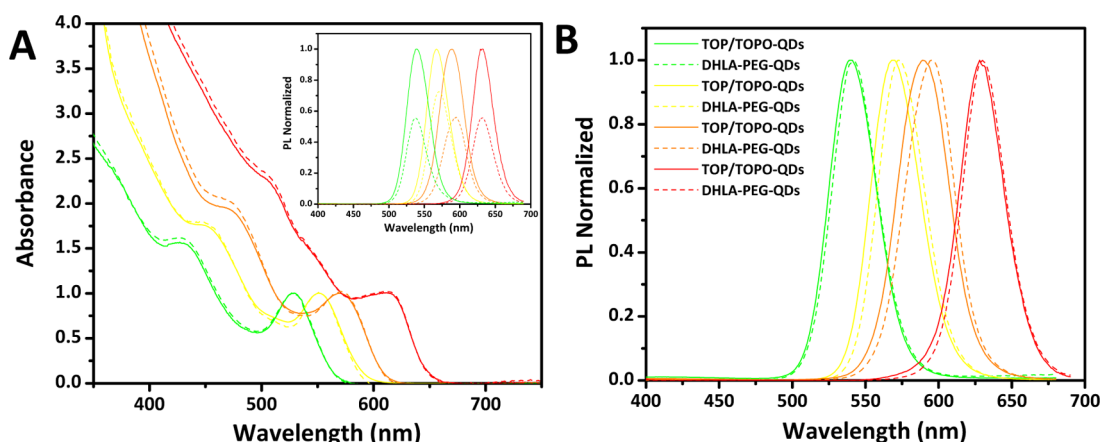


**Figure 2.** (A) Normalized absorption (with respect to the band edge peak) and (B) PL spectra (normalized with respect to the peak value) of the QDs before and after cap exchange, using the preirradiated ligands. Green, yellow, orange and red lines correspond to the 540 nm-, 570 nm-, 590 nm- and 630 nm-emitting QDs; the solid and dashed lines designate dispersions in hexane and in DI water, respectively. The inset in (A) shows the PL spectra of QDS after photoligation with LA-PEG<sub>750</sub>-OCH<sub>3</sub> and transfer to water, normalized with respect to the spectra of TOP/TOPO-QDs in hexane; spectra were collected using dispersions having the same optical density at the excitation line  $\lambda_{exc} = 350$  nm.

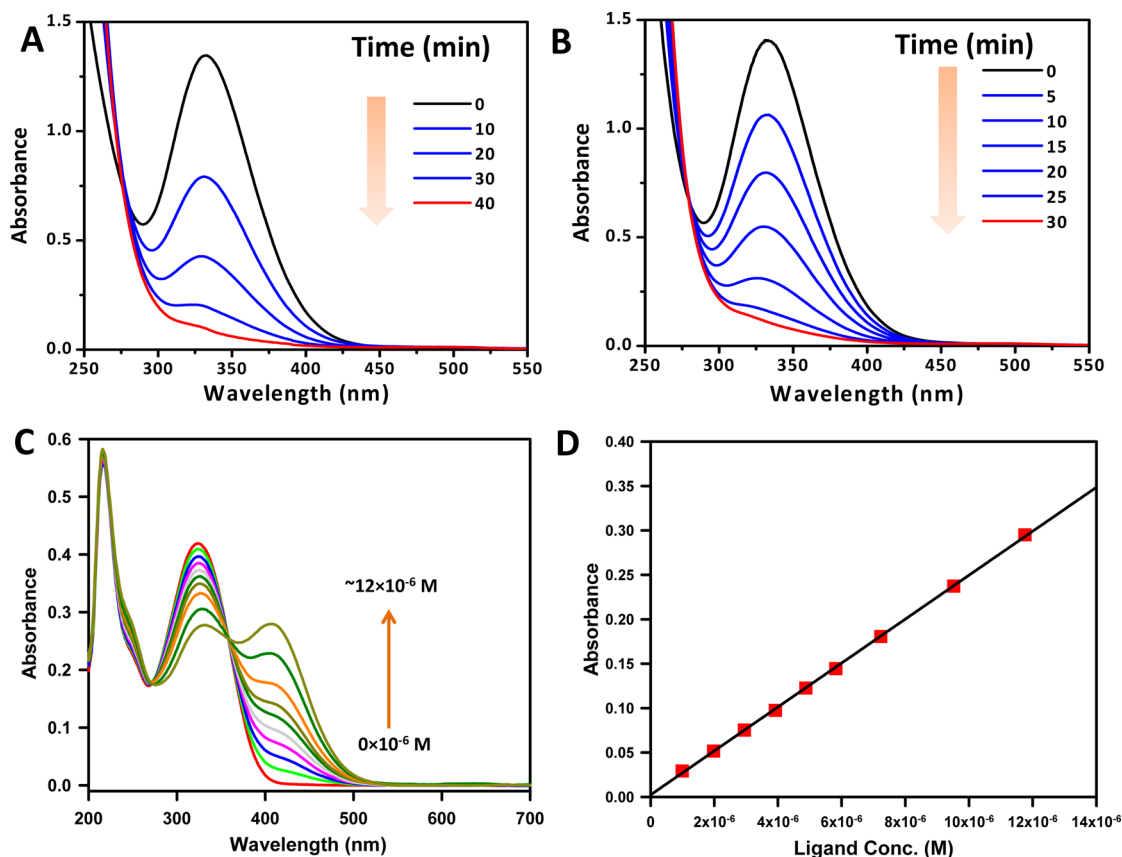


**Figure 3.** Progression of the UV-vis absorption spectra of LA-PEG<sub>750</sub>-OCH<sub>3</sub> dissolved in methanol upon photoirradiation for varying times using (A) sunlight and (B) a UV photoreactor; the ligand concentration was  $\sim 10$  mM. (C) Evolution in the UV spectra of DTNB upon increasing the DHLA-PEG<sub>750</sub>-OCH<sub>3</sub> concentration. (D) Calibration curve showing linear correlation between the absorbance collected at 412 nm and the concentration of DHLA-PEG<sub>750</sub>-OCH<sub>3</sub> used; the concentration of the DTNB reagent was fixed at  $\sim 25$   $\mu$ M in phosphate buffer pH7.8.

dispersions of QDs that are similar to those prepared using borohydride-reduced DHLA (data not shown).

We should note that sunlight irradiation experiments were usually carried out using direct and full exposure to the sun. Experiments carried out during a sunny summer or fall day yielded similar results. Furthermore, we found that experiments carried out during the day but under cloudy conditions also

resulted in an efficient transformation of the ligand after 30–40 min (as verified optically) and a complete ligand exchange when mixed with the QDs; irradiation of a two-phase sample also produced full phase transfer. However, experiments carried out using exposure to sunlight through a laboratory window (still full exposure to light) did not promote complete phase transfer even after several days. Similarly, exposure of a ligand

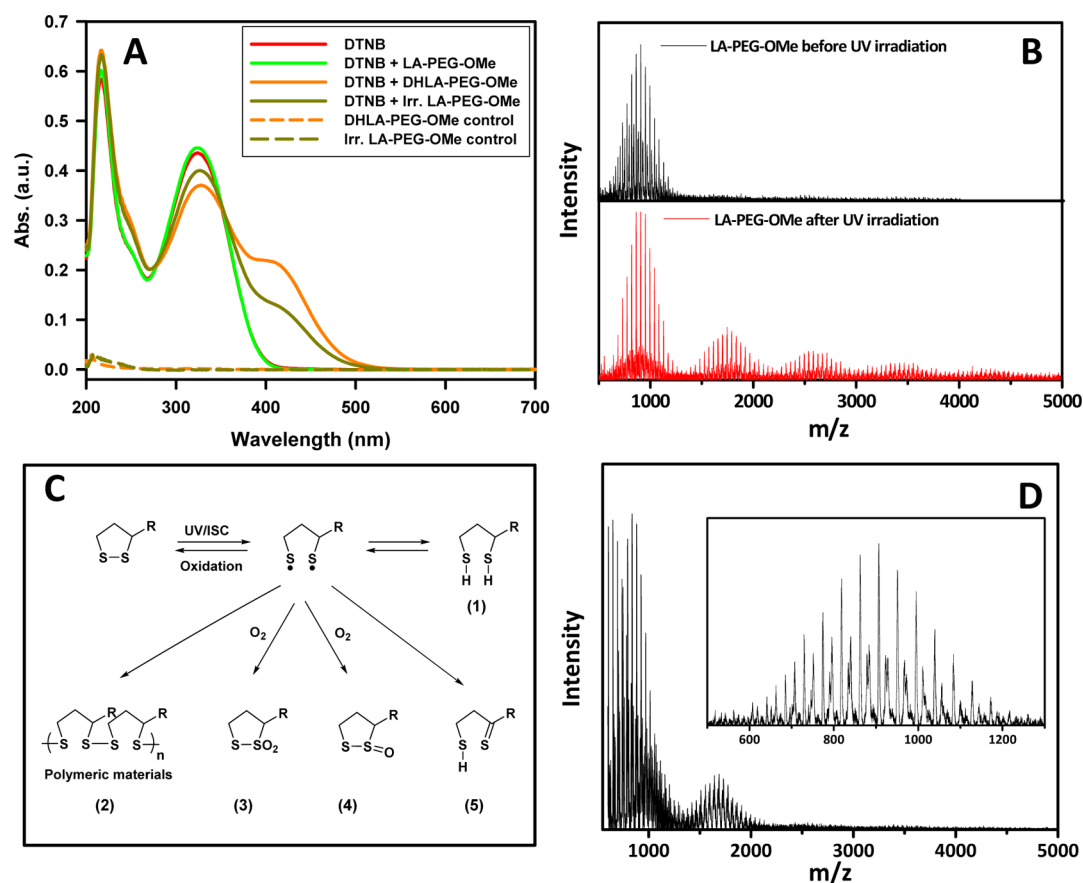


**Figure 4.** (A) UV-vis spectra of the DTNB reagent alone (red line), in the presence of LA-ligands (green line), in the presence of chemically reduced DHLA ligands (orange line), and in the presence of photoirradiated LA-ligands (dark yellow line); also shown are the absorption spectra of pure DHLA-PEG-OMe and UV-irradiated LA-PEG-OMe. Note that the contribution of the LA absorption feature at 335 nm to the spectra is negligible, due to a combination of lower extinction coefficient and smaller concentration of ligands used compared to those of DTNB. The DTNB and PEG-OMe ligand concentrations were  $\sim 25$  and  $\sim 10$   $\mu\text{M}$ , respectively. (B) MALDI mass spectra of the LA-PEG<sub>750</sub>-OCH<sub>3</sub> ligands before (black line) and after UV-irradiation (red line). (C) A few representative UV-induced photochemical transformations of the dithiolane ring are provided based on literature data.<sup>31,40,44,46</sup> The R group can be a short alkyl-COOH, such as for LA, or alkyl-PEG such as the case of the ligands used here. (D) MALDI mass spectra of excess free UV-irradiated LA-PEG<sub>750</sub>-OCH<sub>3</sub> ligands collected in the supernatant after cap exchange.

solution using such conditions did not yield full transformation of the dithiolane groups, where only a small decrease in the absorption feature at 335 nm was measured. This result is attributed to the fact that the glass windows strongly attenuate the UV region of the sun spectrum.

Having demonstrated that the QDs play no direct role in the photochemical transformation of the LA groups and the ensuing ligand exchange, we then centered our effort on monitoring what happens to the LA-based ligands under UV or sunlight irradiation. For this, we systematically characterized the ligands before and after irradiation using UV-vis absorption spectroscopy, Ellman's test/assay and mass spectrometry. These measurements combined allowed us to characterize the nature and relative proportions of some of the photochemically generated species in a pure solution of LA-PEG (or LA) ligands. They also allowed us to gain additional insights into what exactly makes the phase transfer using this photochemical route effective. Figure 3A,B shows the progression of the disulfide absorption band (at 335 nm) upon UV irradiation for 30 min and sunlight exposure for 40 min. A progressive decrease until near complete disappearance in the absorption peak is measured in both cases, a result similar to what we previously reported.<sup>32</sup> This indicates that the photochemical transformation of the ligands is essentially the same, whether

irradiation of the solution is carried in a laboratory set using a UV reactor or simply relying on the UV signal provided by the sun.

We then used the Ellman's assay to quantify the number of available thiol groups in a solution of LA-PEG-OCH<sub>3</sub> following irradiation (via UV or sunlight).<sup>36</sup> Typically, this test relies on the reaction of the reagent 5,5'-dithiobis-2-nitrobenzoic acid (DTNB) with thiol groups in the medium, producing 5-thio-2-nitrobenzoic acid (TNB) that has a distinct absorption signature at 412 nm, manifesting in a color change of the solution to yellow. Quantifying the concentration of thiol groups in the medium was done by comparing the optical data to those collected from a control solutions made of chemically reduced ligand. For this control, a calibration curve using DHLA-PEG-OCH<sub>3</sub> (NaBH<sub>4</sub>-reduced ligand) was generated. As expected, the concentration of thiol groups in a solution of ligand, as indicated by the progression of the signature at 412 nm (ascribed to the TNB product), varied linearly with the concentration of DHLA-PEG-OCH<sub>3</sub> (Figure 3C,D). Furthermore, the slope extracted from that curve should reflect the number of thiol per molecule ( $n$ ) via the relation:  $\text{Abs} = \epsilon \times C \times d \times n$ , where  $\epsilon$  is extinction coefficient of TNB at 412 nm,  $C$  is the molar concentration of DHLA-PEG-OMe, and  $d$  is the optical path of the cell used to collect the absorbance spectra ( $d$

= 1 cm). The experimental slope,  $24,725 \text{ M}^{-1} \times \text{cm}^{-1}$ , was very close to  $2 \times \epsilon(\text{TNB})$ , using  $\epsilon(\text{TNB}) \sim 14,000 \text{ M}^{-1} \times \text{cm}^{-1}$ .<sup>37</sup> This indicates that the chemically reduced ligands essentially yield approximately two thiol groups per ligand, as expected. This curve was used to determine the fraction of thiol groups present in the LA-PEG solution following UV or sunlight irradiation. Figure 4A shows the absorption spectra for DTNB alone, DNTB mixed with LA-PEG<sub>750</sub>-OCH<sub>3</sub>, DNTB mixed with DHLA-PEG<sub>750</sub>-OCH<sub>3</sub>, and DNTB mixed with photoirradiated LA-PEG<sub>750</sub>-OCH<sub>3</sub> at a concentration of 2  $\mu\text{M}$ . The spectrum of LA-PEG<sub>750</sub>-OCH<sub>3</sub> solution shows no contribution at 412 nm, confirming the absence of thiol groups in the oxidized form of the ligand. The data indicate that in the presence of the modified ligands, a new contribution to the absorption at 412 nm appears for DHLA-PEG and photoirradiated LA-PEG; these two solutions also turn yellow. However, the absorption value at 412 nm is  $\sim 2$ -fold larger for DHLA-PEG<sub>750</sub>-OCH<sub>3</sub> than that measured for the photoirradiated ligands, suggesting that species other than DHLA are present. These data support the presence of a significant amount of Ellman's reagent reactive species, presumably thiols, in the irradiated LA-PEG sample, but those species are less abundant than what is measured for the chemically reduced compound.

Further characterization of the molecular species formed during the UV irradiation relied on mass spectrometry measurements. Figure 4B shows the MALDI mass spectra of the LA-PEG<sub>750</sub>-OCH<sub>3</sub> before and after UV-irradiation. The spectrum measured for the oxidized form of the ligand shows only one broad Gaussian peak centered at 900 Da corresponding to the average mass of PEG<sub>750</sub> plus LA; the width reflects the polydisperse nature of the PEG moieties. The set of narrow peaks superposed on top of the main one are spaced by 44 Da, corresponding to the molar mass of ethylene glycol units. The spectrum collected from photoirradiated ligands shows four distinct peaks centered approximately at 900, 1800, 2700, and 3600 Da, indicating the presence of photochemically transformed monomers (as a large fraction), together with higher order oligomers, including dimers, trimers, and tetramers of the transformed ligand. This partial oligomerization upon photoirradiation is consistent with the above data collected from the DTNB assay where lower concentration of thiol groups present in the medium (inferred from the absorption at 412 nm), since the LA-derived molecules in the polymer would not react with DTNB.

To complement the above MALDI data collected from the LA-PEG<sub>750</sub>-OCH<sub>3</sub> ligand, we characterized the pure LA using ESI mass spectrometry. This experiment was carried out in order to achieve better assignment of the mass peaks and avoid issues associated with peak broadening due to the polydispersity of the PEG chains. The ESI mass spectra of LA before and after irradiation are shown in the Supporting Information (Figure S4). The spectrum collected from the compound before irradiation shows two low molecular weight peaks of 229 and 245, ascribed to mass 206 + 23 and 206 + 39 corresponding to Na and K adducts of LA, respectively. In comparison, the spectrum from the UV-irradiated compound shows around 5 distinct peaks (in addition to the two discussed above), including two centered around 435 and 467 Da ascribed to Na+LA-LA and K+LA-LA-O (+16) dimers, two centered around 641 and 673 Da ascribed to Na+LA-LA-LA and K+LA-LA-LA-O (+16) trimers, and two peaks centered at 847 and 879 Da associated with Na+LA-LA-LA-LA and K+LA-

LA-LA-LA-O (+16) tetramers. The spectrum also shows the presence of two peaks at 1053 and 1085 Da corresponding to Na+LA-LA-LA-LA-LA and K+LA-LA-LA-LA-LA-O (+16) pentamers, along with a weaker peak ascribed to hexamers around 1300 Da; these are higher order complexes of photochemically activated LAs. Our data also confirm the presence of oxidized S–O species (see scheme shown in Figure 4C). They also show that the photochemical transformation of the dithiolane rings is the main promoter of linear or cyclic oligomer formation, independent of the PEG moieties. We should note that this experiment could not be performed using the MALDI-MS because of the interference from the matrix, which shows mass peaks around 300–600 Da.

**Understanding the Photochemical Transformation of the LA-Based Ligands.** LA has attracted great attention in chemistry and biology, due to a combination of photochemical activity, its antioxidant properties, and more recently its ability to promote across cell membrane transport of unmodified substrates.<sup>38,39</sup> The presence of a distorted dithiolane ring in its structure endows LA with a characteristic spectroscopic signature, with the HUMO–LUMO energy difference falling within the UV region of the optical spectrum.<sup>31,32</sup> As a result LA exhibits a well-defined absorption feature at  $\sim 335$  nm and can thus be photochemically excited (and transformed) by UV irradiation.<sup>40,41</sup> UV-induced transformation of LA was first studied by Calvin and co-workers as a model system for primary conversion in photosynthesis,<sup>42</sup> and the chemical reactivity of the compound was subsequently examined using spectroscopic techniques.<sup>43</sup> Cumulatively, these studies combined have shown that following irradiation photochemical transformation of the LA yields several products. For example, Murray and co-workers suggested that LA readily reacts with the singlet oxygen to produce compounds containing S–O and S–(O)<sub>2</sub> groups. The formation of these oxidized products implies that a direct reaction between LA and singlet oxygen takes place, indicating that LA can be a good quencher of singlet oxygen.<sup>44</sup> Photochemical transformation of LA was also studied in various solvents, where the formation of several oligomers byproducts was proposed and discussed.<sup>40,41</sup> A more recent study by Packer and co-workers have reported that UV-induced photodegradation of LA can generate DHLA.<sup>45</sup>

The complete reduction of LA to DHLA requires two electrons and thus cannot readily occur under UV excitation unless a certain reducing reagent is available in the medium. Bucher and Sander proposed three pathways for the diradical decay resulting from S–S homolytic cleavage: ring closure leading back to the precursor LA, 1,4-H shift giving mercaptothioaldehyde derivative, or 1,2-H shift giving mercaptoalkyl thiyl radical (see Figure 4C).<sup>31</sup> They also suggested that these highly reactive dithiyl radicals can lead to DHLA formation following hydrogen abstraction. Based on these photochemical properties, a ring-opening polymerization and copolymerization of LA with 1,2-dithiane have also been examined by Endo and co-workers.<sup>46,47</sup>

Overall, the above studies indicate that irradiation of the disulfide likely results in dithiyl radical formation, which in turn can lead to a variety of byproducts depending on the solvent and concentration of the reactants used. One reaction pathway can lead to linear or cyclic oligomerization through S–S bridging between distinct molecules and their oxidation to form oligomeric molecules in which S–O species are present. Figure 4C summarizes schematically a few representative UV-induced photochemical transformations of the dithiolane ring discussed

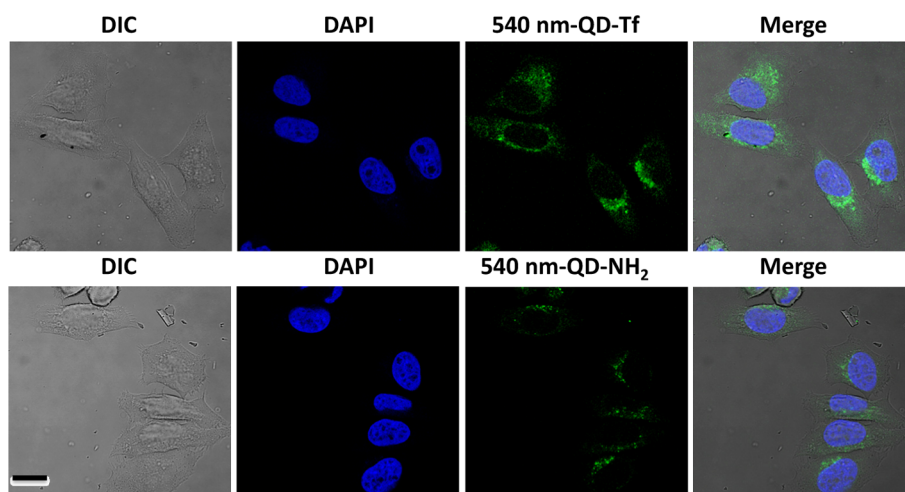


**Figure 5.** (Top) Fluorescence confocal microscopy images of intracellular delivery of green-emitting QD-Tf conjugates into HeLa cells. The panels show DIC image, fluorescence images of cell nuclei stained with DAPI, endosomes stained with QDs-Tf, along with the merged image. The cells were incubated with 200 nM of QDs conjugates at 37 °C for 1 h. (Bottom) Images collected from control cultures incubated with unconjugated QD-PEG-NH<sub>2</sub>. Scale bar = 15 μm.

in the various literature studies. We should note that in addition to those byproducts, cyclic oligomeric disulfides (not depicted in Figure 4) can be formed but would not be reactive toward Ellman's reagent since they have no free thiols; it would thus not contribute to the measured concentrations. However, a linear polymer could have one end reduced to a thiol and the other end oxidized to a sulfonic acid. When LA-compounds are photoexcited and mixed with TOP/TOPO-QDs the above distinct monomeric and oligomeric species compete differently for the nanocrystal surfaces, with stronger coordination anticipated for the oligomers. This can explain why ligation of photochemically transformed LA-PEG ligands requires only 15 min and no additional heat, compared to ligand exchange using the chemically reduced ligands. It is important to note that during exchange, the LA compounds are added in large excess, so minor LA species following photoexcitation could be responsible for the enhanced ligand exchange activity. To confirm this proposed rationale, we characterized the solution of free ligands, collected once ligand exchange of the QDs was complete, using MALDI-MS as above. Briefly, following ligand exchange and solvent evaporation, DI water was added to provide a water dispersion of QDs. The dispersion was purified from excess free ligands using a membrane filtration device with cutoff  $M_w = 50,000$  Da. The filtrate solution containing excess ligands was collected and characterized using MALDI-MS. The spectrum in Figure 4D shows the presence of only monomers and dimers in the retrieved material, and no higher order oligomers were found. In addition, characterization of borohydride-reduced DHLA-PEG ligand showed that only monomers are present (see Supporting Information, Figure S5). This confirms that these polymers are only present upon UV-irradiation of the LA-based ligands.

Together, these findings indicate that these photochemical reactions alter the covalent structure of the dithiolane ring in the LA. They also suggest that the cap exchange process consumes the higher molecular LA species observed by MALDI. It is possible that the high  $M_w$  species are more reactive toward the QD surfaces and facilitate the cap exchange.

**Covalent Conjugation of Photoligated QDs.** Our synthetic scheme allows the *in situ* introduction of functionally heterogeneous LA derivatives onto QD surfaces. This can be

achieved by introducing a small fraction of terminally reactive ligands (e.g., LA-PEG<sub>600</sub>-COOH or LA-PEG<sub>600</sub>-NH<sub>2</sub>) together with the inert one (LA-PEG<sub>750</sub>-OCH<sub>3</sub>) during the photoligation and phase-transfer step.<sup>19</sup> Combining the photoligation strategy with mixed ligand exchange, we prepared two dispersions of reactive nanocrystals. One set was made of QDs exchanged using 10% LA-PEG<sub>600</sub>-amine; the other set has 50% of the surface ligands made of LA-PEG<sub>600</sub>-carboxy. These functionalized QDs were conjugated to the protein transferrin (Tf) and a cell penetrating peptide (CPP), respectively, via carbodiimide coupling; see Experimental Section for more details. Transferrin is a plasma protein present in the blood of mammals and is known to promote intracellular uptake via receptor-mediated endocytosis.<sup>48–50</sup> Conversely, cell penetrating peptides are short amino acid sequences derived from viral proteins and often contain several arginines in their structures (CPP:  $M_w = 1994$  Da).<sup>51</sup> The CPP sequence utilized here (Lys-Trp-Leu-Ala-Aib-Ser-Gly-(Arg)<sub>8</sub>-CONH<sub>2</sub>) was synthesized manually using *in situ* neutralization cycles for Boc solid-phase peptide synthesis following procedures described in the literature.<sup>52,53</sup> These peptides are actively studied by several groups as a means of promoting intracellular uptake of genes and drugs.<sup>54</sup> CPPs are believed to enter cells via direct membrane translocation, though several studies have shown that uptake is also driven by endocytosis.<sup>55</sup>

#### Imaging of Cellular Uptake of Photoligated QDs.

Figure 5 shows the fluorescence confocal images of HeLa cells incubated with QD-Tf conjugates at 37 °C along with cells incubated with dispersions of QD-PEG-NH<sub>2</sub> (control). Shown are side-by-side differential interference contrast (DIC) and fluorescence images corresponding to the distribution of DAPI nuclear staining (blue), 540 nm-emitting QDs (green), along with the merged images. Significant uptake has been observed for the QD-Tf (Figure 5, top). In comparison, weak but not negligible fluorescence was measured for the control culture (Figure 5, bottom). Staining of cells incubated with NH<sub>2</sub>-PEG-coated QDs is not surprising since these amines can promote electrostatic adsorption on the cell membranes followed by endocytosis. This uptake is weaker than that measured for cells incubated with QD-CPP conjugates.<sup>29</sup> Regardless, attaching Tf



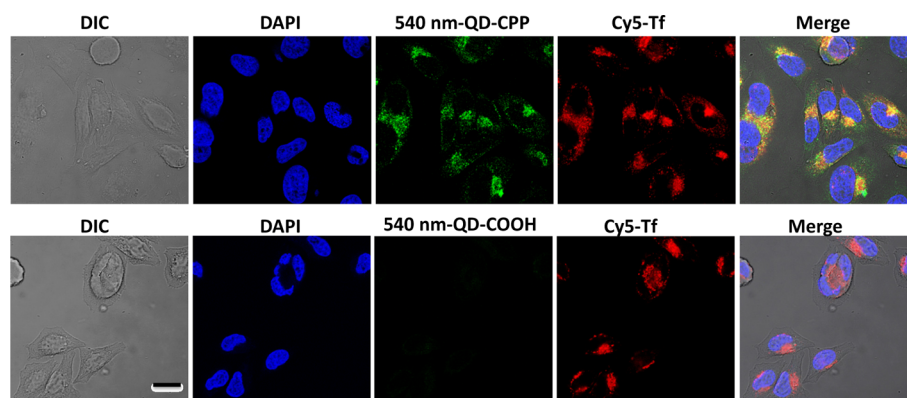


**Figure 6.** (Top) Fluorescence confocal microscopy images of intracellular delivery of green-emitting QD-CPP conjugates into HeLa cells. Representative images showing the corresponding DIC, cell nuclei stained with DAPI, cells labeled with QD-CPP, cells stained with Cy5-Tf (endosome marker), and the merged image. The cells were incubated with 200 nM of QDs conjugates at 37 °C for 1 h. (Bottom) Images collected from control cultures incubated with unconjugated QD-PEG-COOH. Scale bar = 15  $\mu\text{m}$ .

onto the nanocrystals promoted internalization of a much larger amount of QDs.

The panels in Figure 6 show a series of confocal fluorescence images of HeLa cells which have been incubated with QD-CPP conjugates, and carboxy-QDs (unconjugated control), along with the corresponding DIC images. Images corresponding to the fluorescence of DAPI nuclear staining, 540 nm-emitting QD-CPP, Cy5-Tf as endosome marker, along with the merged images are shown. Images show that the presence of CPP promotes high levels of QD-CPP intracellular uptake compared to cells incubated with COOH-QDs (control), with the distribution of QD signal largely being perinuclear and colocalized with that of the Cy5-Tf marker. These findings confirm that the QDs were taken up via endocytosis as shown in previous reports.<sup>56</sup> These data combined prove that ligand exchange and phase transfer of QDs mediated by photochemical transformation of the LA-PEG ligands provide hydrophilic and easy to functionalize QDs, with similar properties to those shown previously using chemically reduced ligands. The resulting materials can be effectively conjugated to biomolecules via easy to implement coupling chemistry, providing fluorescent platforms that can potentially be used in array of imaging and sensing studies.

## CONCLUSION

Photoligation of multidentate LA-modified ligands onto ZnS-overcoated QDs is a greatly promising and easy to implement strategy to transfer these materials from hydrophobic to polar media; it provides homogeneous water dispersions of bioactive QDs. In this study, we combined a few experimental rationales to develop an understanding of the photochemical processes driving this ligation. We tested the effects of irradiating the ligands *in situ* (mixed with the hydrophobic QDs) versus *ex situ* (prior to mixing with the QDs) on the ligand photochemical transformation and the ensuing phase transfer. We used UV-vis absorption spectroscopy, Ellman's assay, MALDI-MS, and ESI-MS to gain additional insights into what makes this photochemically driven phase transfer so effective. We found that ligand exchange does not depend on the mode of irradiation used, as ligands irradiated *ex situ* then mixed with the hydrophobic QDs rapidly ligate on the nanocrystals and promote their phase transfer. We also showed that photoligation is not limited to using a laboratory UV reactor, as transformation of the ligands and the ensuing phase

transfer can be achieved using sunlight. The photochemical transformation produces a heterogeneous mixture of LA derivatives that have significant reactivity toward Ellman's reagent and that contain higher order oligomers, including dimers, trimers, and tetramers as detected by MALDI MS. When mixed with hydrophobic QDs, these compounds compete for coordination on the nanocrystal surfaces, with different affinities; faster and stronger coordination of dimers, trimers, and tetramers on the QD takes place compared to monomers. We also showed that the UV and sunlight irradiation of LA-based ligands provided QDs that are easy to couple with biomolecules such as proteins and peptides, with conjugates exhibiting biological activities identical to those prepared using QDs capped with borohydride-reduced ligands.

The insights gained into understanding what parameters control the photochemical transformation of the ligands and how ligation onto the nanocrystals proceeds, are greatly informative. Ligands play a major role in the overall behavior of colloidal nanocrystals; they control colloidal stability, reactivity and, in certain instances, strongly affect the electronic and spectroscopic behavior of the nanocrystals. This implies that photochemical processes occurring at the interface between inorganic nanomaterials and ligands are complex and may yield new and unexplored phenomena; thus they should further be explored. Furthermore, photoligation of QDs combined with the ability to design various multidentate LA-modified ligands provides fluorescent and compact nanoparticles with great potential for use in imaging, tracking, and sensing.

## EXPERIMENTAL SECTION

**Reagents.** The  $\pm\alpha$ -lipoic acid (LA), poly(ethylene glycol) ( $M_w \sim 600$ ), poly(ethylene glycol) methyl ether ( $M_w \sim 750$ ), methanesulfonyl chloride (99.7%), triphenylphosphine (99%), 4-(*N,N*-dimethylamino)pyridine (DMAP) (99%), triethylamine, sodium borohydride, *N,N*-dicyclohexylcarbodiimide (DCC), succinic anhydride, 1-ethyl-3-(3-(dimethylamino)propyl) carbodiimide hydrochloride (EDC), *N*-hydroxysuccinimide (98%) (NHS), human Transferrin (Tf), 5,5'-dithiobis-2-nitrobenzoic acid (DTNB), NaOH, KOH, NaHCO<sub>3</sub>, organic solvents (THF, CHCl<sub>3</sub>, etc.), and salts (e.g., NaCl, Na<sub>2</sub>SO<sub>4</sub>) were purchased from Sigma-Aldrich Chemicals (St. Louis, MO). Sodium azide (99%), *N,N*-dimethyl-1,3-propanediamine (99%), and 1,3-propane sultone (99%) were purchased from Alfa Aesar (Ward Hill, MA). Deuterated solvents were purchased from Cambridge Isotope Laboratories (Andover, MA). Sulfo-Cy5 NHS



ester was purchased from Lumiprobe (Hallandale Beach, FL). The chemicals and solvents were used as purchased unless otherwise specified. Column purification chromatography was performed using silica gel (60 Å, 230–400 mesh, from Bodman Industries, Aston, PA). PD10 columns were purchased from GE Healthcare (Piscataway, NJ).

**Instrumentation.** The optical absorption measurements were carried out using a Shimadzu UV–vis absorption spectrophotometer (UV 2450 model from Shimadzu). The emission and excitation spectra were collected on a Fluorolog-3 spectrometer (HORIBA Jobin Yvon Inc., Edison, NJ) equipped with PMT detector. The UV-irradiation experiments were performed using a photoreactor (Luzchem UV lamp, Model LZC-4 V) containing 14 lamps, installed on top (6 lamps) and the two sides (4 lamps each). MALDI-MS experiments were conducted using a Bruker MALDI-TOF mass spectrometer. The ESI-MS experiments on LA before and after UV irradiation were carried out using an Exactive plus Orbitrap instrument (from Thermo Scientific).

**Ligand and CdSe-ZnS QD Synthesis.** Three poly(ethylene glycol)-appended lipoic acid (LA-PEG) ligands were prepared and used in this study. One was terminated with an inert OCH<sub>3</sub>, LA-PEG<sub>750</sub>-OCH<sub>3</sub> (PEG  $M_w$  = 750 Da); one was terminated with a COOH, LA-PEG<sub>600</sub>-COOH; and the third was terminated with NH<sub>2</sub>, LA-PEG<sub>600</sub>-NH<sub>2</sub> (PEG  $M_w$  = 600 Da). They were synthesized and characterized, following previous reports.<sup>19,24,25</sup> LA-Zwitterion (LA-ZW) was also prepared, purified and characterized following previous protocols.<sup>20</sup> Finally, four different sets of CdSe-ZnS core-shell QDs emitting at 540 nm (green), at 570 nm (yellow), at 590 nm (orange), and at 630 nm (red) were prepared and used. The QD growth was carried out by reacting organometallic precursors at high temperature in a coordinating solvent mixture made of tri-*n*-octylphosphine (TOP), tri-*n*-octylphosphine oxide (TOPO), and alkylamine, in two steps: growth of CdSe cores followed by overcoating with 5–6 monolayers of ZnS.<sup>6,13–15,18</sup>

**Photochemical Ligation of QDs.** In a typical reaction, 150  $\mu$ L of CdSe-ZnS QDs (20  $\mu$ M) was precipitated with ethanol twice using a scintillation vial and then dispersed in 750  $\mu$ L of *n*-hexane (the final QD concentration = 3  $\mu$ M). In a separate vial equipped with a magnetic stirring bar, 47 mg of LA-PEG<sub>750</sub>-OCH<sub>3</sub> ligands were dissolved in 500  $\mu$ L of MeOH (~100 mM). The ligands were irradiated in the UV photoreactor ( $\lambda_{\text{irr}}$  maximum peak at 350 nm and a power of 4.5 mW/cm<sup>2</sup>) or under sunlight for 30 min, followed by the addition of a small amount of tetramethylammonium hydroxide (~5 mM). The QDs in hexane were added to the ligand solution and stirred for 15 min at room temperature. The organic solvents (hexane and methanol) were removed under vacuum, followed by redispersion of the QDs in ethanol mixed with a small amount of chloroform. Hexane was slowly added until the solution became turbid. Following centrifugation, the supernatant was removed, the content mildly dried under vacuum for ~5 min, and buffer was added to disperse the QDs. The aqueous dispersion of QDs was filtered through a 0.45  $\mu$ m syringe filter and further purified from free ligands by applying three rounds of concentration/dilution using a membrane filtration device (Amicon Ultra 50,000  $M_w$ , from Millipore). The QDs were finally dispersed in DI water or buffer and stored at 4 °C for later use. We should note that the above procedure has also been applied to QDs photoligated with LA-ZW ligands.<sup>32</sup> Here too the cap exchange could be carried out *in situ* (i.e., irradiation of the ligands in the presence of QDs) or *ex situ* using either a UV photoreactor or under sunlight exposure.

The functionalization of QDs with carboxyl- or amine-terminated ligands was achieved by introducing a small fraction of reactive ligands (LA-PEG<sub>600</sub>-COOH or LA-PEG<sub>600</sub>-NH<sub>2</sub>) along with LA-PEG<sub>750</sub>-OCH<sub>3</sub> (inert ligand) at the desired molar ratios prior to the cap exchange step. Here, we prepared two aliquots of green-emitting QDs; one was functionalized with 10% PEG-amine and the other had 50% PEG-carboxyl. These were used for further coupling to Tf and cell penetrating peptides (see below).

**Quantification of Thiol Groups Using Ellman's Test.** Two stock solutions in phosphate buffer (containing 1.0 mM EDTA, pH 7.8) were prepared, one made of 1.0 mM DTNB and the other made of 0.2 mM DHLA-PEG<sub>750</sub>-OCH<sub>3</sub>. Then, solutions of varying

concentrations of DHLA-PEG<sub>750</sub>-OCH<sub>3</sub> and a fixed concentration of DTNB were prepared by adding (to a total volume of 2 mL PBS buffer) 50  $\mu$ L of 1.0 mM DTNB (above) and various aliquots of 0.2 mM DHLA-PEG<sub>750</sub>-OCH<sub>3</sub> solution. The final concentration of DHLA-PEG-OME in the solutions varied from  $1 \times 10^{-6}$  to  $11.8 \times 10^{-6}$  M, while that of DTNB was maintained at ~24–25  $\mu$ M (i.e., excess DTNB). The EDTA was added as bivalent metal scavenger to prevent impurity metal catalyzed oxidation of free (reduced) sulfhydryls in the medium, i.e., impurity metals can form chelates with EDTA present in the solution (<https://www.piercenet.com/instructions/2160311.pdf>). The mixture was left reacting for 15 min before collecting an absorption spectrum for each concentration used. Plotting the absorption value at 412 versus ligand concentration provided a linear (standard) curve, with a slope that is proportional to the anticipated number of thiol groups per molecule/ligand,  $n$  (i.e., slope =  $\epsilon(\text{TNB}) \times d \times n$ ). In addition, we carried out side-by-side comparison of the absorption spectra collected from solutions of DTNB mixed with either DHLA-PEG-OME or UV-irradiated (for 30 min) LA-PEG-OME at the same molar concentration. Comparing the absorption values at 412 nm collected from both solutions allowed us to extract an estimate for the concentration of free thiol groups in the solution of irradiated ligands compared to the one prepared with borohydride-reduce ligands (DHLA-PEG-OME).

**Sample Preparation for MALDI Mass Spectrometry.** The matrix was prepared as follows: 10 mg of 3,5-dimethyl-4-hydroxycinnamic acid was dispersed in 0.7 mL of MeOH containing 0.7  $\mu$ L of TFA (trifluoroacetic acid). A separate solution containing 0.3  $\mu$ L of TFA in 0.3 mL of water was also prepared. The two solutions were mixed for 10 min, precipitated, and then centrifuged for ~1–2 min at 3600 rpm. The precipitate was discarded, and the supernatant was used as the MALDI matrix. An aqueous dispersion (10  $\mu$ L, 50 mM) of LA-PEG<sub>750</sub>-OCH<sub>3</sub> ligands, with or without UV-irradiation, was added to 90  $\mu$ L of the above MALDI matrix solution. Then, 2  $\mu$ L of the mixture was deposited on the MALDI target plate and air-dried. The sample was irradiated at 337 nm using an N<sub>2</sub> pulsed laser. In general, the data collected from 1000 laser pulses were averaged to obtain the final spectrum.

**Preparation of QD-Transferrin (QD-Tf) Conjugates.** Transferrin (0.25 mg/mL) in PBS buffer (10 mM, pH = 7.4) was first activated using 10,000 equiv of EDC (1-ethyl-3-(3-(dimethylamino)propyl) carbodiimide) and NHS (*N*-hydroxysuccinimide) for 30 min. QD-PEG-NH<sub>2</sub> (200  $\mu$ L of 3  $\mu$ M stock solution) was added in 800  $\mu$ L of PBS buffer (10 mM, pH = 8.4). Then, the QD solution was added dropwise, and the mixture was stirred for 4 h at room temperature; the final QD:Tf molar ratio used was 1:5. The QD-Tf conjugates were purified by size exclusion chromatography using a PD10 column (GE healthcare), then characterized by UV–vis absorption spectroscopy.

**Preparation of QD-Cell Penetrating Peptide (QD-CPP) Conjugates.** COOH-PEG-capped QDs (300  $\mu$ L of 3  $\mu$ M stock solution) were first activated using 10,000 equiv of EDC (1-ethyl-3-(3-(dimethylamino)propyl) carbodiimide) and NHS (*N*-hydroxysuccinimide) in 700  $\mu$ L PBS buffer (10 mM, pH = 7.4) for 30 min. Cell penetrating peptide (3  $\mu$ L, 7.2 mM in water) were diluted in 100  $\mu$ L of PBS buffer (pH = 8.4), and slowly added to the QD dispersion, and the mixture was stirred for 4 h at room temperature; the final QD:CPP molar ratio used was 1:25. The QD-CPP conjugates were purified using PD10 column and characterized as done above for the QD-Tf Conjugates.

**Cell Culture.** HeLa cell lines were provided by the FSU cell culture facility. The cells were cultured in complete growth medium (Dulbecco's modified eagle's medium, DMEM, Corning Cellgro) supplemented with 4.5 g/L glucose, L-glutamine, sodium pyruvate, 1% (v/v) antibiotic-antimycotic 100 $\times$  (Gibco), 1% (v/v) nonessential amino-acid solution 100 $\times$  (Sigma), and 10% (v/v) fetal bovine serum (FBS, from Gibco). Cells were grown as a monolayer in T25-flasks at 37 °C under a humidified 5% CO<sub>2</sub> atmosphere. Subconfluent cells (~60%) were detached every 2–4 days using trypsin-EDTA (Invitrogen).

**Cellular Delivery of QD-CPP or QD-Tf Conjugates.** The  $8 \times 10^4$  cells were seeded onto 18 mm circle microcover glasses placed into 24-

well microtiter plates (CellStar, VWR), and the plates were placed in an incubator overnight to allow attachment and recovery. After 24 h, given amounts of QD-PEG-NH<sub>2</sub>, QD-PEG-COOH, QD-Tf, or QD-CPP bioconjugates, diluted into culture medium (DMEM without phenol red, Invitrogen) to the desired concentration (200 nM), were added to the cell culture and then incubated for 1 h at 37 °C. Cy5-Tf marker (at 40 μg/mL) was also added to the culture to label the late endosomal compartments. Excess unbound QD reagents and Cy5-Tf were removed by washing three times with phosphate-buffered saline (PBS, pH = 7.4). The cells were then fixed in 3.7% paraformaldehyde for 12 min at room temperature, washed, and mounted in ProLong Antifade mounting media containing DAPI dye (Invitrogen) for nuclear staining, then imaged using confocal microscopy.

**Cellular Imaging.** Laser-scanning confocal microscopy images shown in Figures 5 and 6 were collected using a Leica TCS SP2 DM6000 microscope equipped with a Leica 63× oil immersion objective (NA = 1.4), available at the FSU School of Medicine. Blue DAPI and green fluorescence of the QDs were excited using a 405 nm diode laser, and the emissions were detected using an Acoustic Optical Tunable Filter (AOTF) and the ranges of 436–477 nm and 506–556 nm, respectively. The red fluorescence from Cy5-Tf was excited using a 633 nm HeNe laser, and the emission was detected in the range of 663–705 nm also using an AOTF.

## ■ ASSOCIATED CONTENT

### ● Supporting Information

Additional experimental details on the UV–vis and PL spectra of QDs prepared using sunlight irradiation or the UV photoreactor and using LA-ZW ligands, along with the MALDI-MS collected from chemically reduced LA-PEG ligands and ESI-MS spectra collected from LA ligand before and after UV irradiation. This material is available free of charge via the Internet at <http://pubs.acs.org>.

## ■ AUTHOR INFORMATION

### Corresponding Author

\*mattoussi@chem.fsu.edu

### Notes

The authors declare no competing financial interest.

## ■ ACKNOWLEDGMENTS

We thank FSU and the National Science Foundation (NSF-CHE, no. 1058957) for financial support. We would also like to thank Mr. Walter Hammack and Dr. Mark Crosswhite from the Department of Agriculture and Consumer Services (FDACS), Tallahassee, for their assistance with the ESI experiments. We are grateful to Naiqian Zhan and Dinesh Mishra at FSU for the helpful discussions and material support.

## ■ REFERENCES

- (1) Wu, X. Y.; Liu, H. J.; Liu, J. Q.; Haley, K. N.; Treadway, J. A.; Larson, J. P.; Ge, N. F.; Peale, F.; Bruchez, M. P. *Nat. Biotechnol.* **2003**, *21*, 41.
- (2) Michalet, X.; Pinaud, F.; Bentolila, L.; Tsay, J.; Doose, S.; Li, J.; Sundaresan, G.; Wu, A.; Gambhir, S.; Weiss, S. *Science* **2005**, *307*, 538.
- (3) Mattoussi, H.; Palui, G.; Na, H. B. *Adv. Drug Delivery Rev.* **2012**, *64*, 138.
- (4) Kay, E. R.; Lee, J.; Nocera, D. G.; Bawendi, M. G. *Angew. Chem., Int. Ed.* **2013**, *52*, 1165.
- (5) Cassette, E.; Helle, M.; Bezdetsnaya, L.; Marchal, F.; Dubertret, B.; Pons, T. *Adv. Drug Delivery Rev.* **2013**, *65*, 719.
- (6) Dabbousi, B. O.; RodriguezViejo, J.; Mikulec, F. V.; Heine, J. R.; Mattoussi, H.; Ober, R.; Jensen, K. F.; Bawendi, M. G. *J. Phys. Chem. B* **1997**, *101*, 9463.

- (7) Aldeek, F.; Balan, L.; Medjahdi, G.; Roques-Carmes, T.; Malval, J. P.; Mustin, C.; Ghanbaja, J.; Schneider, R. *J. Phys. Chem. C* **2009**, *113*, 19458.
- (8) Medintz, I. L.; Uyeda, H. T.; Goldman, E. R.; Mattoussi, H. *Nat. Mater.* **2005**, *4*, 435.
- (9) Aldeek, F.; Mustin, C.; Balan, L.; Medjahdi, G.; Roques-Carmes, T.; Arnoux, P.; Schneider, R. *Eur. J. Inorg. Chem.* **2011**, 794.
- (10) Reiss, P.; Protiere, M.; Li, L. *Small* **2009**, *5*, 154.
- (11) Alivisatos, A. P. *Science* **1996**, *271*, 933.
- (12) Leatherdale, C. A.; Woo, W. K.; Mikulec, F. V.; Bawendi, M. G. *J. Phys. Chem. B* **2002**, *106*, 7619.
- (13) Murray, C. B.; Norris, D. J.; Bawendi, M. G. *J. Am. Chem. Soc.* **1993**, *115*, 8706.
- (14) Peng, Z. A.; Peng, X. G. *J. Am. Chem. Soc.* **2001**, *123*, 183.
- (15) Qu, L. H.; Peng, Z. A.; Peng, X. G. *Nano Lett.* **2001**, *1*, 333.
- (16) Talapin, D. V.; Rogach, A. L.; Kornowski, A.; Haase, M.; Weller, H. *Nano Lett.* **2001**, *1*, 207.
- (17) Hines, M. A.; Guyot-Sionnest, P. *J. Phys. Chem.* **1996**, *100*, 468.
- (18) Talapin, D. V.; Lee, J. S.; Kovalenko, M. V.; Shevchenko, E. V. *Chem. Rev.* **2010**, *110*, 389.
- (19) Mei, B. C.; Susumu, K.; Medintz, I. L.; Delehanty, J. B.; Mountziaris, T. J.; Mattoussi, H. *J. Mater. Chem.* **2008**, *18*, 4949.
- (20) Park, J.; Nam, J.; Won, N.; Jin, H.; Jung, S.; Cho, S. H.; Kim, S. *Adv. Funct. Mater.* **2011**, *21*, 1558.
- (21) Liu, W. H.; Greytak, A. B.; Lee, J.; Wong, C. R.; Park, J.; Marshall, L. F.; Jiang, W.; Curtin, P. N.; Ting, A. Y.; Nocera, D. G.; Fukumura, D.; Jain, R. K.; Bawendi, M. G. *J. Am. Chem. Soc.* **2010**, *132*, 472.
- (22) Mattoussi, H.; Mauro, J. M.; Goldman, E. R.; Anderson, G. P.; Sundar, V. C.; Mikulec, F. V.; Bawendi, M. G. *J. Am. Chem. Soc.* **2000**, *122*, 12142.
- (23) Susumu, K.; Uyeda, H. T.; Medintz, I. L.; Pons, T.; Delehanty, J. B.; Mattoussi, H. *J. Am. Chem. Soc.* **2007**, *129*, 13987.
- (24) Uyeda, H. T.; Medintz, I. L.; Jaiswal, J. K.; Simon, S. M.; Mattoussi, H. *J. Am. Chem. Soc.* **2005**, *127*, 3870.
- (25) Mei, B. C.; Susumu, K.; Medintz, I. L.; Mattoussi, H. *Nat. Protoc.* **2009**, *4*, 412.
- (26) Susumu, K.; Oh, E.; Delehanty, J. B.; Blanco-Canosa, J. B.; Johnson, B. J.; Jain, V.; Hervey, W. J.; Algar, W. R.; Boeneman, K.; Dawson, P. E.; Medintz, I. L. *J. Am. Chem. Soc.* **2011**, *133*, 9480.
- (27) Muro, E.; Pons, T.; Lequeux, N.; Fragola, A.; Sanson, N.; Lenkei, Z.; Dubertret, B. *J. Am. Chem. Soc.* **2010**, *132*, 4556.
- (28) Howie, J. K.; Houts, J. J.; Sawyer, D. T. *J. Am. Chem. Soc.* **1977**, *99*, 6323.
- (29) Liu, W.; Howarth, M.; Greytak, A. B.; Zheng, Y.; Nocera, D. G.; Ting, A. Y.; Bawendi, M. G. *J. Am. Chem. Soc.* **2008**, *130*, 1274.
- (30) Smisman, E. E.; Sorenson, J. R. *J. Org. Chem.* **1965**, *30*, 4008.
- (31) Bucher, G.; Lu, C. Y.; Sander, W. *ChemPhysChem* **2005**, *6*, 2607.
- (32) Palui, G.; Avellini, T.; Zhan, N.; Pan, F.; Gray, D.; Alabugin, I.; Mattoussi, H. *J. Am. Chem. Soc.* **2012**, *134*, 16370.
- (33) Zhan, N. Q.; Palui, G.; Safi, M.; Ji, X.; Mattoussi, H. *J. Am. Chem. Soc.* **2013**, *135*, 13786.
- (34) Zhan, N.; Palui, G.; Grise, H.; Tang, H.; Alabugin, I.; Mattoussi, H. *ACS Appl. Mater. Interfaces* **2013**, *5*, 2861.
- (35) Liu, W. H.; Choi, H. S.; Zimmer, J. P.; Tanaka, E.; Frangioni, J. V.; Bawendi, M. G. *J. Am. Chem. Soc.* **2007**, *129*, 14530.
- (36) Ellman, G. L.; Courtney, K. D.; Andres, V.; Featherstone, R. M. *Biochem. Pharmacol.* **1961**, *7*, 88.
- (37) Riener, C. K.; Kada, G.; Gruber, H. *J. Anal. Bioanal. Chem.* **2002**, *373*, 266.
- (38) Bang, E.-K.; Gasparini, G.; Molinard, G.; Roux, A.; Sakai, N.; Matile, S. *J. Am. Chem. Soc.* **2013**, *135*, 2088.
- (39) Gasparini, G.; Bang, E.-K.; Molinard, G.; Tulumello, D. V.; Ward, S.; Kelley, S. O.; Roux, A.; Sakai, N.; Matile, S. *J. Am. Chem. Soc.* **2014**, *136*, 6069.
- (40) Brown, P. R.; Edwards, J. O. *J. Org. Chem.* **1969**, *34*, 3131.
- (41) Brown, P. R.; Edwards, J. O. *J. Chromatogr.* **1969**, *43*, 515.
- (42) Bartrop, J. A.; Hayes, P. M.; Calvin, M. *J. Am. Chem. Soc.* **1954**, *76*, 4348.

- (43) Wagner, A. F.; Walton, E.; Boxer, G. E.; Pruss, M. P.; Holly, F. W.; Folkers, K. *J. Am. Chem. Soc.* **1956**, *78*, 5079.
- (44) Stary, F. E.; Jindal, S. L.; Murray, R. W. *J. Org. Chem.* **1975**, *40*, 58.
- (45) Matsugo, S.; Han, D.; Tritschler, H. J.; Packer, L. *Biochem Mol. Biol. Int.* **1996**, *38*, 51.
- (46) Endo, K.; Yamanaka, T. *Macromolecules* **2006**, *39*, 4038.
- (47) Kisanuki, A.; Kimpara, Y.; Oikado, Y.; Kado, N.; Matsumoto, M.; Endo, K. *J. Polym. Sci., Part A: Polym. Chem.* **2010**, *48*, 5247.
- (48) Yang, P. H.; Sun, X. S.; Chiu, J. F.; Sun, H. Z.; He, Q. Y. *Bioconjugate Chem.* **2005**, *16*, 494.
- (49) Qian, Z. M.; Li, H. Y.; Sun, H. Z.; Ho, K. *Pharmacol Rev.* **2002**, *54*, 561.
- (50) Kibel, A.; Belovari, T.; Drenjancevic-Peric, I. *Med. Hypotheses* **2008**, *70*, 793.
- (51) Torchilin, V. P. *Adv. Drug Delivery Rev.* **2008**, *60*, 548.
- (52) Schnolzer, M.; Alewood, P.; Jones, A.; Alewood, D.; Kent, S. B. *H. Int. J. Pept. Protein Res.* **1992**, *40*, 180.
- (53) Delehanty, J. B.; Medintz, I. L.; Pons, T.; Brunel, F. M.; Dawson, P. E.; Mattoussi, H. *Bioconjugate Chem.* **2006**, *17*, 920.
- (54) Wadia, J. S.; Dowdy, S. F. *Curr. Opin. Biotechnol.* **2002**, *13*, 52.
- (55) Jiao, C. Y.; Delaroche, D.; Burlina, F.; Alves, I. D.; Chassaing, G.; Sagan, S. *J. Biol. Chem.* **2009**, *284*, 33957.
- (56) Delehanty, J. B.; Bradburne, C. E.; Boeneman, K.; Susumu, K.; Farrell, D.; Mei, B. C.; Blanco-Canosa, J. B.; Dawson, G.; Dawson, P. E.; Mattoussi, H.; Medintz, I. L. *Integr. Biol.* **2010**, *2*, 265.